Modelling Orientation Preference Structure by Minimizing Wirelength in a Cortical Circuit for Contour Completion

by

Sangh S. Gautam

B.E., Electronics and Communication, Netaji Subhas Institute of Technology, 1998

THESIS

Submitted in Partial Fulfillment of the
Requirements for the Degree of

Master of Science
Computer Science

The University of New Mexico

Albuquerque, New Mexico

May 2004

Dedication

To my parents, Bhooley Singh Gautam and Bimlesh Gautam, for their support and encouragement for carrying out this thesis and to my friends at UNM who provided the help and environment for carrying out this work.

"It is the tension between creativity and skepticism that has produced the stunning and unexpected finding of science" – Carl Sagan

Acknowledgments

I would like to thank my advisor, Professor Lance Williams, for his support and guidance. I would also like to thank the open source project for providing much needed tools to the academic community. I also want to thank the CS department's staff for answering all my queries with a smile. Lastly, I want to thank my family for being understanding and supportive through the effort.

Modelling Orientation Preference Structure by Minimizing Wirelength in a Cortical Circuit for Contour Completion

by

Sangh S. Gautam

ABSTRACT OF THESIS

Submitted in Partial Fulfillment of the
Requirements for the Degree of

Master of Science
Computer Science

The University of New Mexico

Albuquerque, New Mexico

May 2004

Modelling Orientation Preference Structure by Minimizing Wirelength in a Cortical Circuit for Contour Completion

by

Sangh S. Gautam

B.E., Electronics and Communication, Netaji Subhas Institute of Technology, 1998

M.S., Computer Science, University of New Mexico, 2004

Abstract

Orientation preference maps of simple cells in the visual cortex have been studied as part of the process of understanding human vision. Iso-orientation bands arranged in pinwheels with adjacent pinwheels having opposite signed spin are the most striking feature of the orientation map. The phenomenon of illusory contours has been modelled by completion field theory which uses *a priori* probabilities based on a distribution of all possible completion curves. It is hypothesized that the simple cells form a circuit to calculate a distribution corresponding to the most probable contour completions. It is proposed that the embedding of simple cells in the visual cortex minimizes the wirelength of this circuit. A side effect is the formation of pinwheels or singularities in the orientation preference map. Preference maps synthesized using this theory show the existence of pinwheels but the spin of the pinwheels does

not vary probably due to the use of a hexagonal sampling pattern which is not two colorable, to sample the visual space.

Contents

List of Figures

Chapter 1

Introduction

1.1 Overview

The structure and function of the human visual system has long intrigued scientists and philosophers. Although a lot is known about the anatomy of the visual system, *e.g.*, the structure of the eye, neurons, and those parts of the brain concerned with vision, the interactions of processes and information being passed from one part to another has remained elusive. The most common observations about the visual system were formulated by psychologists as Gestalt laws of perception. In this process several vision illusions were also studied like Necker cube, Muller-Lyer and Saw tooth illusions. Subsequently, it was observed that the visual system also exhibited a tendency to form illusory contours. The most striking example is probabily the Kanizsa triangle, shown in Figure 1.1. Neuroscientists on the other hand were able to find the response of neurons in the visual system evoked by a specific stimulus. It was observed that the response of simple cells in the cortex formed patterns on the visual cortex. These were termed *cortical maps*. Different properties of the stimuli, like orientation and position, formed different preference maps. This work

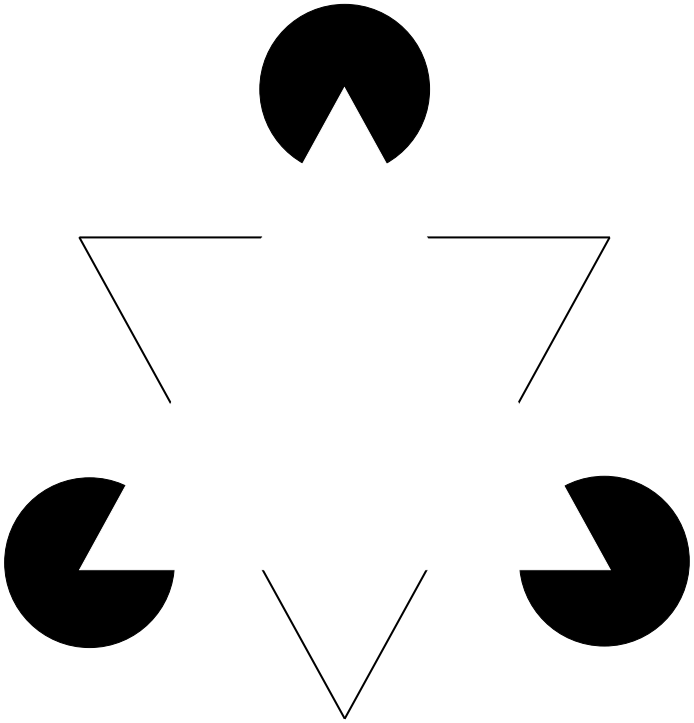

Figure 1.1 Kanizsa triangle: Illusion of one triangle over another.

is an attempt to explain the appearence of orientation preference cortical maps by a model which assumes that the spatial layout of simple cells minimizes the total wirelength of cortical circuit for contour completion.

1.2 Illusory contours

Illusory contours are constructs of the visual system which correspond to object boundaries which do not objectively exist. Horn (1980) [6] tried to explain this effect by using the concept of minimum *bending energy*. Grossberg *et al.* (1985) [5] and Zucker *et al.* (1989) [14] describe repeated convolution models and neural network algorithms respectively to synthesize illusory contours. One of the important works

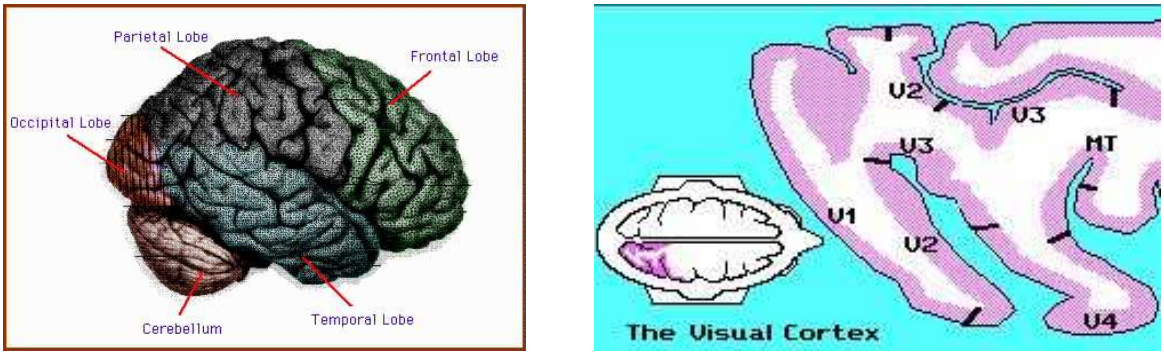

(a) (b)

Figure 1.2 (a) Lobes of cerebral cortex, (b) Location of *visual cortex* or *Area V1*.

in this area and the most pertinent to this thesis is the *stochastic completion field* model of Williams and Jacobs (1997) [18]. The basic idea is to represent the family of curves joining two points as a prior distribution of completion shapes characterized using a random walk. Section 3.1 explains this theory in detail.

1.3 Cortical maps

Cerebral cortex is the convoluted external surface of the brain, Figure 1.2(a). As shown in Figure 1.2(b), it is divided into four lobes: *frontal, parietal, temporal and occipital*. Certain areas of the cortex are also divided into primary, secondary and tertiary areas based on their direct processing of sensory information. One of the largest of these areas is known as *primary visual cortex* or *Area V1*, and is located in the occipital lobe.

Experimenting on cats, Hubel and Weisel in [7] and [8] observed that specific neurons, called *simple cells*, in the Area V1 of cats responded to bars of light at specific locations and orientations in the visual field. The area of the visual field

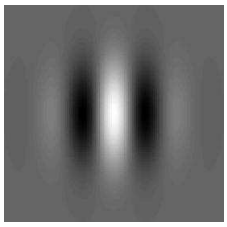

Figure 1.3 Gabor function representation of the receptive field.

which evoked a response was mapped and was termed a *receptive field*. The advent of modern techniques like optical imaging and microelectrode recording allowed better characterization of the receptive field. It was found that the receptive field consists of alternating regions of excitory and inhibitory response, as shown in Figure 1.3. Researchers like Daughman [3] have modelled the response using the $2D$ Gabor functions, which is the product of a sinusoid of a particular frequency and orientation, and a Gaussian envelope. It is defined as follows:

$$G(x, y, \sigma, \omega, \theta, \phi) = \sin(\omega\ (x\ \cdot\ \cos\theta - y\ \cdot\ \sin\theta) + \phi)\ \cdot\ e^{\frac{(x-x_0)^2+(y-y_0)^2}{2\sigma^2}}$$

where x_0 and y_0 specify the mean and σ specifies the standard deviation of the Gaussian. ω determines frequency, θ determines angle of orientation and ϕ is the phase of the sinusoid.

Experiments with receptive fields also allowed researchers to observe the spatial distribution of these parameters on the surface of the visual cortex. Maps based on orientation, spatial position, ocular dominance, etc. were studied. Of all the maps, orientation preference maps, and spatial position maps are most relevant to us. It was found that simple cells exhibit pinwheel like singularities in their orientation preference map but that visual space is represented continuously.

The most significant observation made by Hubel and Weisel was that simple cells exhibit orientation preference, *i.e.*, simple cells are narrowly tuned to orientation and

position of the stimulus. This orientation was found by observing only the orientation parameter of the receptive field. The orientation preference varies gradually across the surface of the cortex in a pattern termed a *cortical map*. Modern techniques like optical imaging confirm the earlier findings and show clearly that these orientation preference maps are organized as pinwheels.

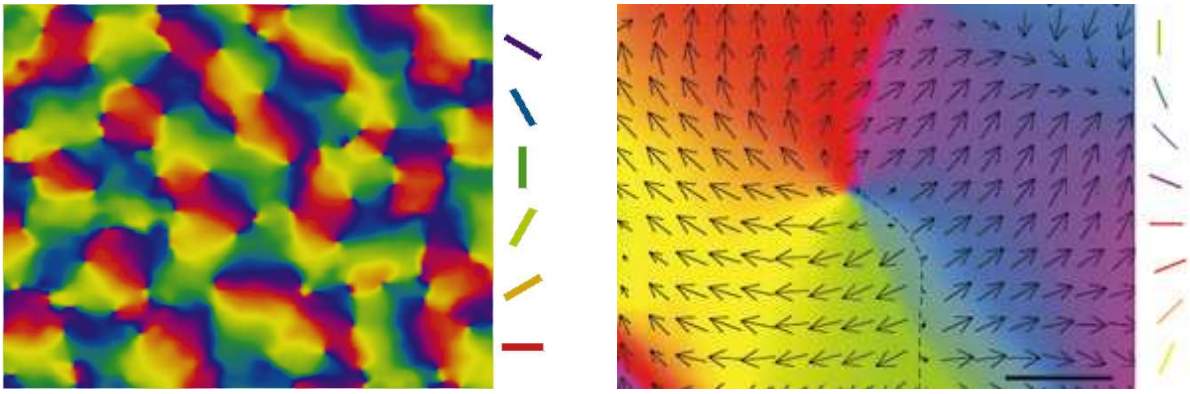

(a) (b)

Figure 1.4 (a) Orientation preference map has adjacent pinwheels with opposite spins [1](b) Single pinwheel with clockwise spin.[1].

As evident in Figure 1.4, the orientation preference maps exhibit two important characteristics:

- The iso-orientation domains converge at singularities termed *pinwheels*.
- Pinwheels are defined to have a spin according to the orientations arranged in the pinwheel. It can be observed that the adjacent pinwheels have opposite spins, and thus form iso-orientation domains.

Subsequent to this discovery many theories were proposed to explain the pinwheel structure. Durbin Mitchison [4] suggested it is the result of dimensionality

reduction, *i.e.*, from N-dimensions (where N depends on many properties like orientation, spatial position, ocular dominance, etc.) to the two-dimensional surface of the visual cortex while trying to maximize the continuity of the feature maps. In terms of the Gabor function this is equivalent to representing $\mathbb{R}^2$ (coordinate) $\times\mathbb{R}^2$ (coordinate) $\times S^1$ (orientation) $\times S^1$ (phase) $\times\mathbb{R}^2$ (width, length) onto $\mathbb{R}^2$ (2D visual cortex). Swindale [17] models this map based on mathematical topology using the Klein bottle. He also theorized that the appearence of the feature maps is due to the smooth representation and uniform coverage of every stimulus of the signal [16]. Wire length minimization approaches claim that the map is a result of minimizing total wire length of a cortical circuit connecting pairs of simple cells. Recently Koulokov and Chlovskii [10] used the wire length minimization approach to generate artificial maps using connections based on a Gaussian random variable in the difference in orientation preference of pairs of simple cells.

A significant amount of research has been done to explain orientation preference maps, and there is a general consensus on the pinwheel pattern. It is also accepted that spatial preference maps vary continuously in both x and y coordinates as shown in Figure 1.5. This thesis is based on a model where simple cells are tuned to discrete orientations and positions, and are used to compute a distribution of curves termed a *stochastic completion field*. Simple cells are connected to each other based on the probability that points are part of the boundary of a single object. The orientation and spatial preference maps which minimize total connection wire length in this cortical circuit are computed.

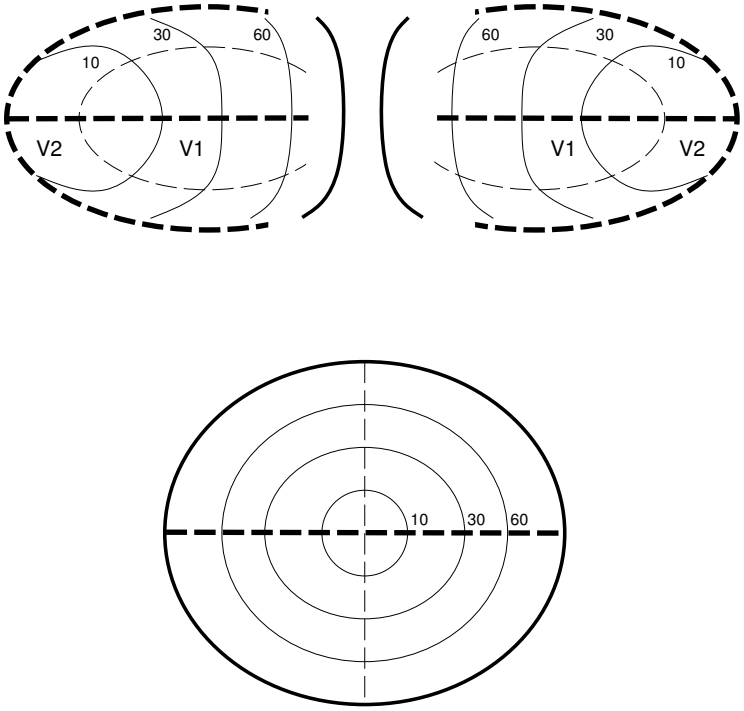

Figure 1.5 The upper two figures show the continuous position preference map on the left and right side of the cerebral cortex. The lower figure displays the visual field being mapped on the cortex.

Chapter 2

Koulakov's wire length minimization approach

2.1 Overview

The brain is a result of million years of evolution. In the course of that process, it has gone through natural selection and tuned itself better to meet the essential requirements of mammals. Therefore it is safe to hypothesize that the optimization of neural wiring could be a crucial factor in the placement of neurons in the visual cortex. Recently Koulakov *et al.* [10] synthesized artificial orientation preference map by minimizing the total inter-neuron connection length. Their model consists of a square lattice of N neurons with periodic boundaries. Each neuron has a preferred orientation. It follows that the properties of a neuron are governed by its preferred orientation and the connections it receives from other neurons.

In Koulakov's *et al.'s* model, the number of connections of a neuron with other

neurons depends on the connection function $C(\Delta\theta)$:

$$C(\Delta\theta) = A \cdot e^{\frac{\Delta\theta^2}{2a^2}} + B \ .$$

where $\Delta\theta$ is the difference in orientation preference between the two neurons. For different values of A, B, and width, a, they produced different orientation preference maps they termed *salt and pepper*, *stripes* and *pinwheels*. The matrix of connections between the N neurons was represented as a binary two-dimensional matrix of size $N \times N$. The total connection length L is then:

$$L = \sum_{i,j=1}^{N} R_{ij} M_{i \leftarrow j}.$$

It is minimized using simulated annealing (explained in Section 4). Koulakov *et al.* change the orientation preference of each neuron iteratively by the value $\Delta\theta$, which is distributed exponentially. At each iteration, for each neuron, n_1, with preferred orientation θ_1, $C(\theta_1 - \theta_2)$ number of connections are made with the closest neurons having preferred orientation, θ_2. Note that n_1 is also connected with neurons of all possible preferred orientations, θ_2, in this fashion. Total wire length, or energy, is calculated, and the preferred orientation change is accepted or rejected according to the Metropolis scheme [13].

2.2 Results

The uniform connection function results in a *salt and pepper* organization of the orientation map. This is expected, since neurons of all the orientations are connected in equal numbers. *Ice cubes*, *stripe* and *wavy ice cube* organizations are produced for a Gaussian connection function. Figure 2.1-2.6 display Koulakov *et al.'s* results.

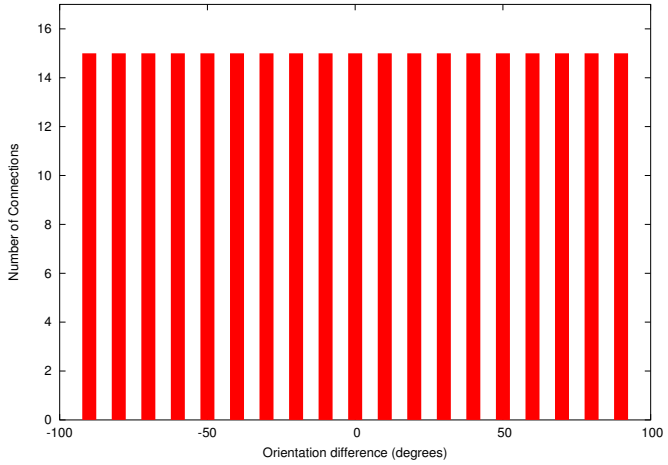

Figure 2.1 Uniform connection function (replotted from [10]).

As the width of the Gaussian envelope, denoted by a in the connection function, decreases, the orientation map varies from an ice cube organization to a layout which more closely resembles pinwheels.

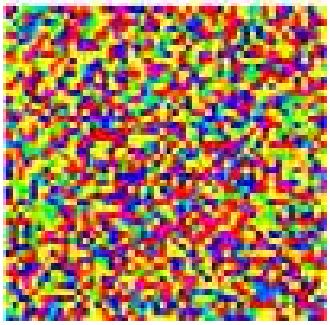

Figure 2.2 Salt and pepper organization for orientation preference map from [10](corresponding to the connection function in Figure 2.1).

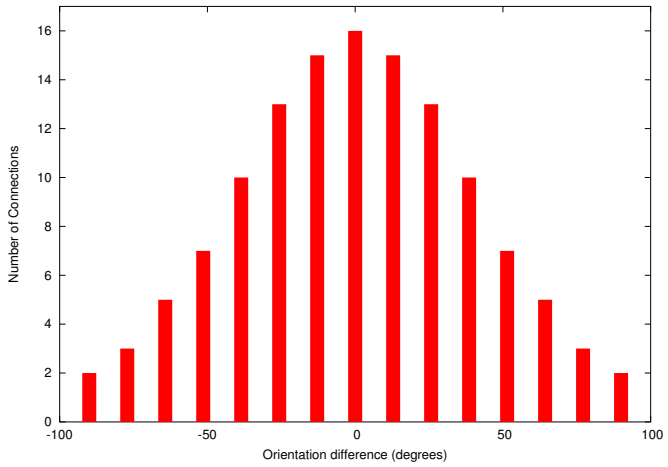

Figure 2.3 Connection function (replotted from [10]).

2.3 Critique

The following points stand out from the Koulakov *et al.* model:

- ***Connection function:*** Unfortunately the choice of a Gaussian connection function is completely arbitrary. Marr [12] argues that a vision model should not only reproduce results, but also be able to explain the theory or underlying

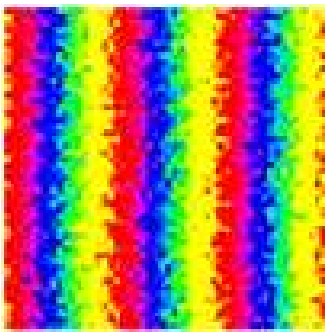

Figure 2.4 Stripes organization for orientation preference map from [10](corresponding to the connection function in Figure 2.3).

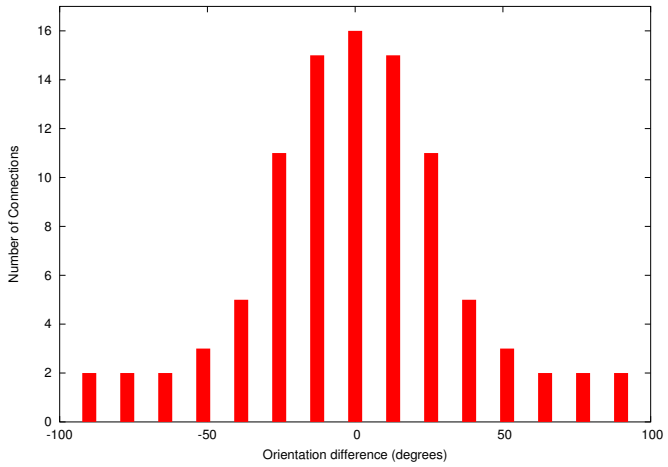

Figure 2.5 Connection function (replotted from [10]).

computation behind a model. In this case the inherent theory behind the choice of cortical circuit is missing. Ideally, this choice should be a part of a larger theory of vision explaining the purpose of the connection function. In Koulakov's work, even a hint of such a theory is missing. In Marr's [12] own words Koulakov has attempted "to *describe* the behavior of cells, but not to *explain* such behavior".

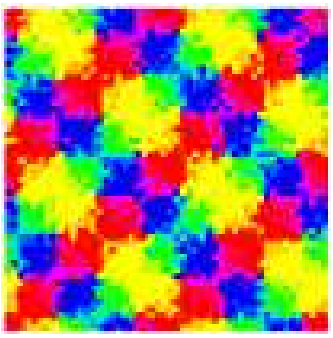

Figure 2.6 Pinwheels organization for orientation preference map from [10] (corresponding to connection function in Figure 2.5).

- ***Spatial cortical map:*** The spatial position preference is also an important property of simple cells and Koulakov *et al.* completely ignore this property.

Chapter 3

Illusory contour and stochastic completion fields

3.1 Stochastic completion fields

Williams and Jacobs [18]introduced the concept of *stochastic completion fields* in an attempt to explain the phenomenon of illusory contours. The main ideas are :

- A particle's state is composed of its direction and position ($\mathbb{R}^2 \times S^1$). Its trajectory in this space is determined by a random walk in direction.
- A *decay constant*, τ, is used to model the distribution of trajectory lengths.
- This process, described by Williams and Jacobs [18] is Markov.
- The position and orientation of the particle are updated as follows:

$$\dot{x} = \cos\theta$$

$$\dot{y} = \sin\theta$$

$$\dot{\theta} = N(0, \sigma^2).$$

- The equation of motion defines the change in a particle's direction of motion and position as a function of time while the decay constant prevents infinite lifetimes for the particles, since after some amount of time all particles will decay.

- The aim is to find the probability that a particle starting in state (x_p, y_p, θ_p), undergoing a random walk in direction, passes through state (u, v, ϕ) on its way to final state (x_q, y_q, θ_q). The starting state is termed a *source* and the final state a *sink*.

- The *source field* is defined as $P(x, y, \theta \mid 0, 0, 0)$ *i.e.* the probability that a particle at source $(0, 0, 0)$ reaches (x, y, θ) before it decays. If G' is the *Green's function*, then the source field is computed using the following equation:

$$P(u, v, \phi \mid 0, 0, 0) = \int_{-\infty}^{+\infty} dx \int_{-\infty}^{+\infty} dy \int_{-\pi}^{\pi} d\theta \, G(u', v', \phi') P(x, y, \theta; 0) \cdot e^{\frac{-t}{\tau}}.$$

  where

$$u' = (u - x) \cos\theta + (v - y) \sin\theta$$

$$v' = -(u - x) \sin\theta + (v - y) \cos\theta$$

$$\phi' = \phi - \theta.$$

- Source fields with different characteristics can be generated using different values for three parameters *speed* γ, *halflife* τ and *diffusivity* σ^2. Figures 3.1-3.3 show source fields for different values of the parameters, τ and γ.

- Similarly a *sink field*, $q(u, v, \phi)$, is defined as the probability that a particle at (u, v, ϕ) reaches the sink state .

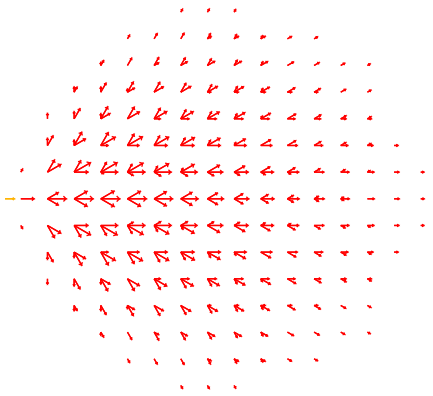

Figure 3.1 Source field diagram: $\gamma^2 = 0.64,\ \tau = 1.0$.

- Consequently the *completion field*, $C(u, v, \phi)$, is defined as the probability that a particle starting in state p ends at state q while passing through state (u, v, ϕ). Because of the Markov property, it is the product of the source and sink field.

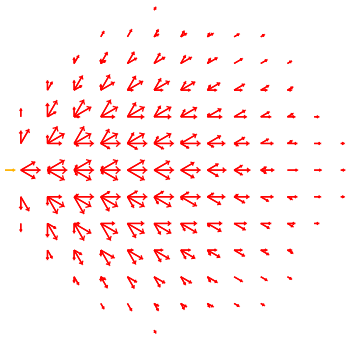

Figure 3.2 Source field diagram: $\gamma^2 = 0.16,\ \tau = 100.0$.

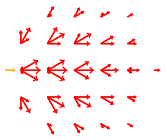

Figure 3.3 Source field diagram: $\gamma^2 = 0.04,\ \tau = 10.0$.

In [18] the particle motion statistics are displayed as source field, sink field, and completion field diagrams. As shown in Figures 3.1-3.3, in the source field diagram, a particle starts from the state (0,0,0) and slowly decays. Arrows are displayed at a position representing the probability that the particle passes through that position. The length of each arrow is proportional to the probability and the direction indicated by the arrow indicates the direction of the particle's motion. Sink field diagrams and

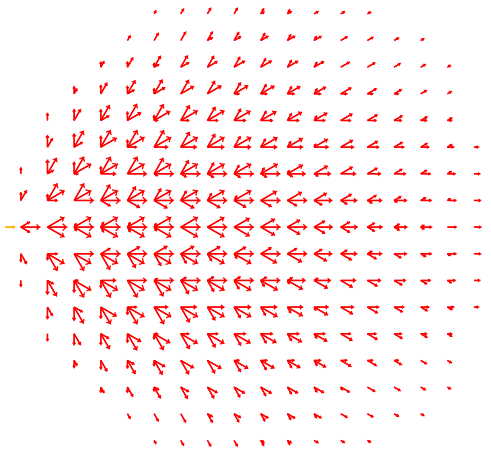

Figure 3.4 Source field diagram: $\gamma^2 = 0.36,\ \tau = 50.0$.

completion field diagrams display the same information using the same convention.

Chapter 4

Technical preliminaries

4.1 Basics

One of the intentions of Williams and Jacobs [18] was the possibility of explaining the activity of neurons with receptive fields tuned to specific orientations and positions, as a representation of the stochastic completion field. According to them, neurons or simple cells might be representing local image plane statistics of this distribution. This thesis is an effort to explore this hypothesis. The following definitions and assumptions are key to the thesis:

- Visual space ($\mathbb{R}^2 \times S^1$), is the cartesian product of ordinary x-y space where each position is defined by $\mathbb{R}^2$, and S^1 space, *i.e.*, θ direction. Cortical space is defined as $\mathbb{R}^2$, *i.e.*, ordinary x-y space, where every position is occupied by a single simple cell.

- A *simple cell*, in our formalism, is a simplification of real simple cells in Area V1. It is assumed to be tuned to a single orientation and position in visual space. Therefore each *simple cell* is uniquely identified by its visual space

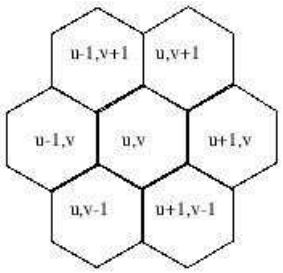

Figure 4.1 Hexagonal coordinate system

position and orientation preference.

- Source, sink, and completion fields, described earlier, are functions of the visual space, $(\mathbb{R}^2 \times S^1)$. Analogous to the field diagram, a kernel diagram is used to depict the connection characteristics of a simple cell. A binary connection function (explained in Section 4.2) is used to connect 2 simple cells when some probability, defined in Section 3.1, is above a threshold. The *kernel diagram* displays the visual space position and orientation characteristics of simple cell to which a second simple cell is connected. Since the connection function is binary, the length of the arrow displays whether a connection is present or not. Figure 5.8 shows a typical kernel diagram. The probability of a connection (described in Section 4.2) depends on the differences in positions and orientations of the two simple cells it connects.

- A Hexagonal coordinate system [15] is used, since it is the highest order tesselation of the $\mathbb{R}^2$ plane. Figure 4.1 displays this coordinate system.

- The optimization problem addressed in this thesis belongs to the category of combinatorial optimization problems. For a grid with N simple cells there are $N!$ possible embeddings. Each embedding takes $O(N^2)$ time complexity to compute the wire length of the embedding on the cortical circuit. Therefore the total complexity is $O(N^{2N!})$. It is clearly intractable to enumerate all of these

embeddings, therefore simulated annealing is used for finding the embedding which minimizes the wire length.

- **Simulated Annealing:**

  In 1983, Kirkpatrick *et al.* [9] proposed the concept of *simulated annealing*. The Metropolis Monte-Carlo scheme [13] is a standard method for solving combinatorial optimization problems of this sort. It has been used to solve optimization problems of large scale like the traveling salesman problem and the layout of integrated circuits. As described in [13], the Metropolis algorithm needs the following elements:

  - **System configuration:** N simple cells, each tuned to a single position and orientation in visual space, are assigned positions in the cortical space.
  - **Random change generator:** Two simple cells are chosen at random and swapped according to the Metropolis scheme.
  - **Minimization Function *E*** The total wire length (Section 4.2) of the cortical circuit embedded in the cortical space.
  - **Annealing schedule:** As defined in Metropolis scheme, a variable T is chosen as the *temperature* of the system. This is decreased by a constant factor in every iteration.

  The essence of the algorithm is to attempt random exchanges, at a temperature T, in the configuration and always accept those changes which decrease the energy function, E, of the system. Those changes which increase the energy function are accepted with a probability p where:

  $$p = e^{-\frac{\Delta E}{T}}.$$

- Typically a 1mm square of visual cortex contains 100,000 neurons. It is not feasible to optimize a grid with that many neurons due to limitations in computation resources and time.

- To eliminate boundary effects, we employ periodic boundaries. To achieve this effect, the cortical space is considered as a *torus*. Figure 4.2 shows the effect of these conditions in the kernel diagram. The cortical space is also represented by a torus for the same reason.

4.2 Details

As described in Section 3.1, the Green's function, $G(x_p, y_p, \theta_p, x_q, y_q, \theta_q \ ; \ t)$, is the probability of a random walk of length, t, starting at (x_p, y_p, θ_p) and ending at (x_q, y_q, θ_q). The Green's function is the solution of the differential equation, more specifically, a Fokker-Planck's equation [19] with an impulse function as the initial condition. The equation describes the motion of an ensemble of particles moving in direction undergoing Brownian motion. The product of the Green's function and an exponential decay function is time integrated and is used to define a new Green's function, is as follows:

$$G'(x_p, y_p, \theta_p, x_q, y_q, \theta_q) = \int_0^{+\infty} dt \; G(x_p, y_p, \theta_p, x_q, y_q, \theta_q \ ; \ t) \ \cdot \ e^{\frac{-t}{\tau}}.$$

Now, a cortical circuit of N simple cells is created by connecting any simple cell p to a simple cell q according to the following connection function $C(p, q)$:

$$C(p,q) = \begin{cases} 1 & G(x_p, y_p, \theta_p, x_q, y_q, \theta_q) < \alpha \\ 0 & \text{otherwise} \end{cases}$$

where α is a pre-defined threshold and orientation and spatial preference of neurons p and q is (x_p, y_p, θ_p) and (x_q, y_q, θ_q) respectively. Then the total wire length of the circuit is defined as

$$L = \sum_{i,j=1}^{N} distance(i,j) \times C(i,j)$$

where $distance(i, j)$ is the distance between ith and jth simple cell on the hexagonal grid representing the cortical space. Using simulated annealing, the wire length for

the resulting circuit is minimized and the resulting orientation and spatial preference maps are rendered. Similar to Koulakov *et al.* this thesis is based on the wire length minimization approach, but the connection between two neurons has a probability calculated using the stochastic completion field model. Consequently the connection between two simple cells depends on both their orientations and positions rather then just their orientation as used by Koulakov *et al.*

4.3 Preliminary experiments

As described in Section 3.1 different source fields can be generated by changing any of the three parameters, *i.e.* speed (γ), diffusivity (σ^2) and halflife (τ). To better understand the relationship between γ, σ^2, and the resulting orientation preference maps, a somewhat simpler probability function was initially used. In other words, instead of the Green's function for the Fokker-Planck equation used by Williams and Jacobs [19], a much simpler Gaussian probability function was used. It is assumed that the orientation preference and position preference are independent Gaussian random variables, *i.e.*, the probability of connection between simple cell p and simple cell q is:

$$P(x_p, y_p, \theta_p \mid x_q, y_q, \theta_q) = \frac{1}{\sqrt{8\pi^3 {\sigma_\theta}^2 {\sigma_x}^2 {\sigma_y}^2}} \times e^{\frac{{\theta_p - \theta_q}^2}{2{\sigma_\theta}^2}} \times e^{\frac{{x_A - x_B}^2}{2{\sigma_x}^2}} \times e^{\frac{{y_A - x_B}^2}{2{\sigma_y}^2}}$$

where

- (x_p, y_p, θ_p) is the preference of simple cell p in the $(\mathbb{R}^2 \times S^1)$ space and (x_q, y_q, θ_q) is the preference of simple cell q in the $(\mathbb{R}^2 \times S^1)$ space.
- ${\sigma_\theta}^2$ is the variance of the Gaussian in difference in orientation preference.
- ${\sigma_x}^2$ is the variance of the Gaussian in difference of x axis spatial preference.

- $\sigma_y{}^2$ is the variance of the Gaussian in difference of y axis spatial preference.

4.3.1 Setup

A cortical space of 30 $\times$ 30 simple cells, with a visual space of 10 $\times$ 15 and with 6 different orientation preferences was used. Instead of the previously described criterion of thresholding the probabilities, the number of connections N for each simple cell was used to determine threshold. All the possible connections for each simple cell were sorted and the most probable N number of connections were instantiated.

4.3.2 Results and Conclusion

Different kernels were generated using different values for the variances $\sigma_\theta{}^2$, $\sigma_x{}^2$ and $\sigma_y{}^2$. Initially the simple cells were randomly embedded in the cortical space. The most probable connections were instantiated for each simple cell and then the simulated annealing process was used to embed them subject to the minimum total wire length constraint. This produced orientation and spatial preference maps. Three type of organizations for the orientation preference maps were observed: 1.) *Patches* (Figure 4.5); 2.) *Stripes* (Figure 4.10); 3.) *Salt and pepper* (Figure 4.15).

The following observations concerning the orientation and position preference maps were made:

- **Patches:** From the kernel diagram in Figure 4.4, it seems that the connection threshold function chooses some connections with orientation preference different than that of the source. But from the histogram it is observed that a simple cell connects primarily only with simple cells of similar orientation preference. This explains the patches organization since the probability depends solely on orientation and position preference plays no role. It seems

natural, then, that the optimization process would embed simple cells with similar orientation preference together and this explains the result. The plots of the spatial preference maps strengthen this hypothesis since they do not show any continuous pattern. Hence, it is unlikely that they play any role in the optimization process.

- **Stripes:** From the kernel diagram in Figure 4.9, it is observed that the simple cell's position preference has some influence on the connection characteristics. The histogram further corroborates this since it makes clear that some connections occur with simple cells having orientation preference other than that of the source simple cell. It is interesting to observe that the spatial preference (x axis) map seems to organize as continuous organization, which suggests that the optimization process is probably embedding simple cells, with adjacent spatial preference (especially x axis), close to each other. Therefore a simple cell mostly connects to simple cells of similar orientation preference (within a single iso-orientation stripe). But it also has connections with other simple cells of similar preference in one dimension, namely, x-axis.

- **Salt and Pepper:** From the kernel diagram in Figure 4.14 and the histogram in Figure 4.13, it is clear that the simple cells are connected entirely due to spatial preference since a simple cell connects to simple cells with all orientation preferences indiscriminately. It is observed that both spatial preference diagrams continuously vary. We observe that if both spatial preference maps continuously vary then the orientation preference map will most likely have a salt and pepper organization.

Finally to summarize the effect of orientation and spatial preference, a graph (Figure 4.3.2) was also plotted. It is observed that as the orientation variance σ_θ increases the orientation patterns are more likely to result in a salt and pepper organization. We conjecture that this is because the orientation preference dominates

spatial preference. Similarly, when the spatial preference dominates, *i.e.*, as ${\sigma_x}^2 = {\sigma_y}^2$ is increased, the salt and pepper organization is more likely. It is also observed that the stripes organization represents transition from the patches to the salt and pepper organization.

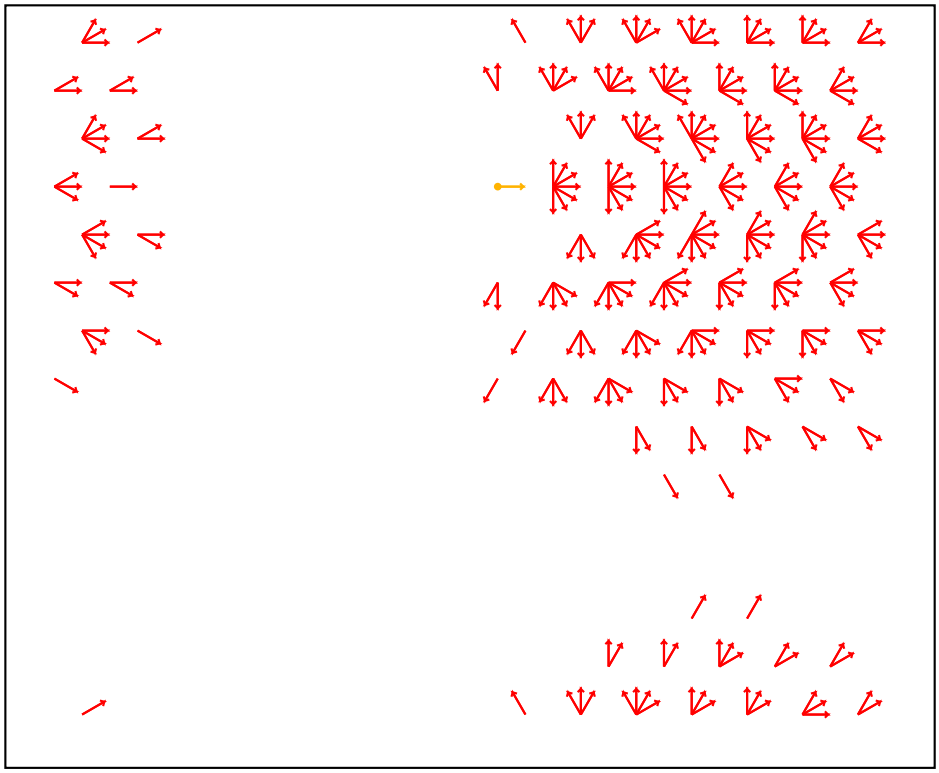

Figure 4.2 Effect of toroidal geometry on the kernel.

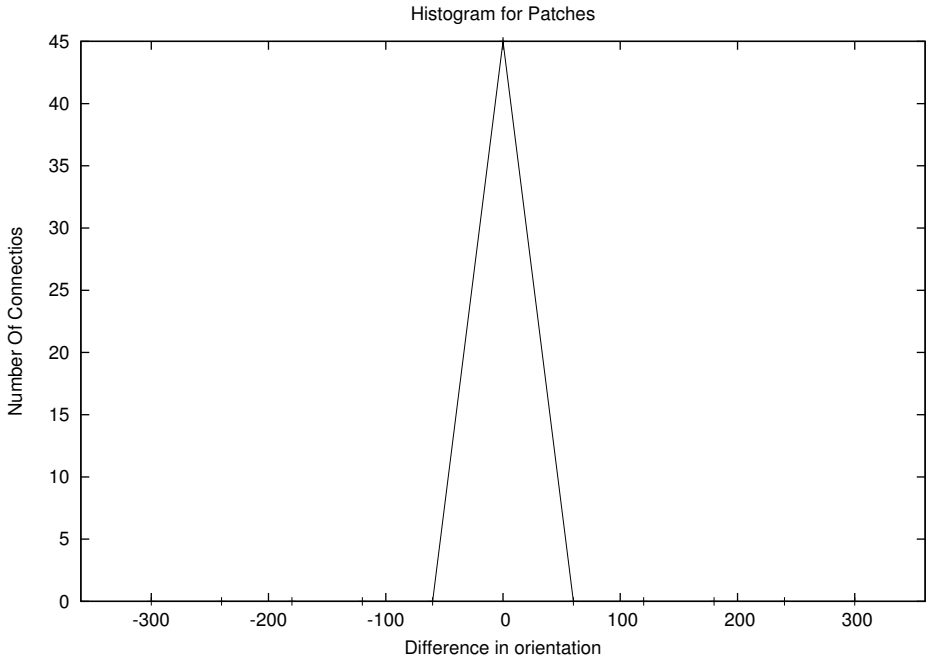

Figure 4.3 Number of connections vs. orientation difference with connecting simple cell for patches organization.

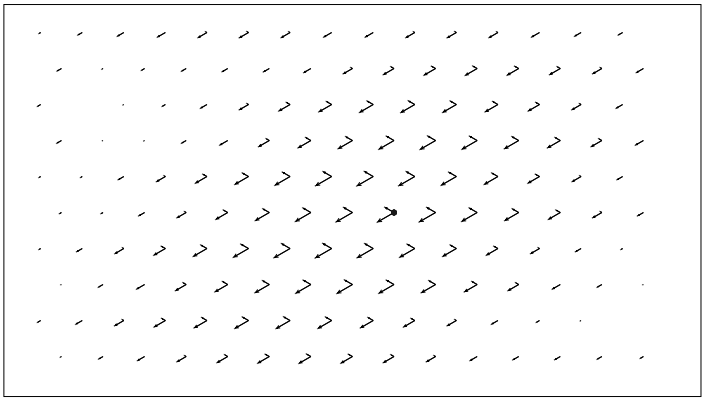

Figure 4.4 Kernel diagram for the experiment yielding the patches organization.

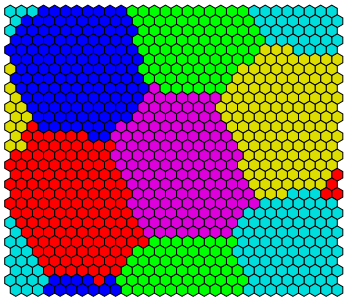

Figure 4.5 Orientation preference map for patches organization.

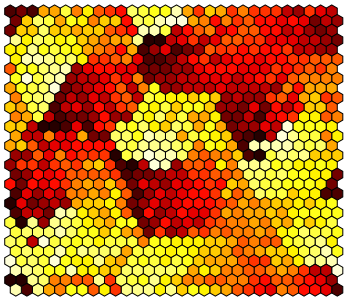

Figure 4.6 Spatial position map (x-axis) for patches organization. We observe a patches like organization.

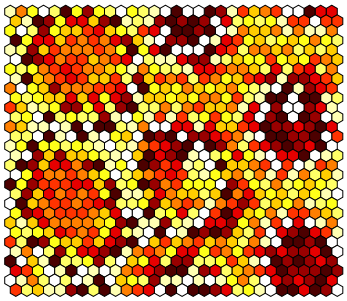

Figure 4.7 Spatial position map (y-axis) for patches organization. We observe a patches like organization.

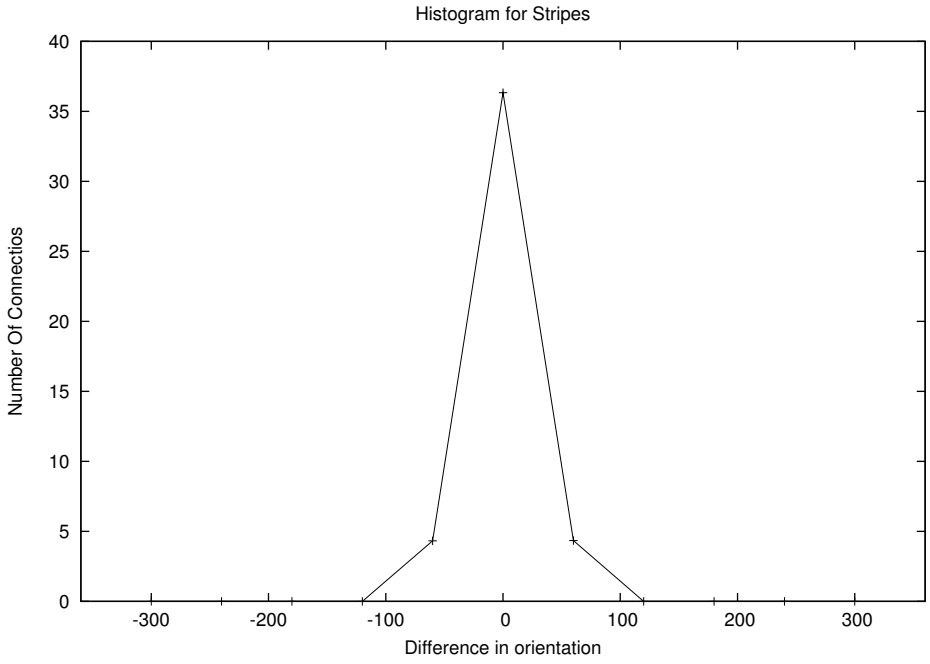

Figure 4.8 Number of connections vs. orientation difference with connecting simple cell for the stripes organization.

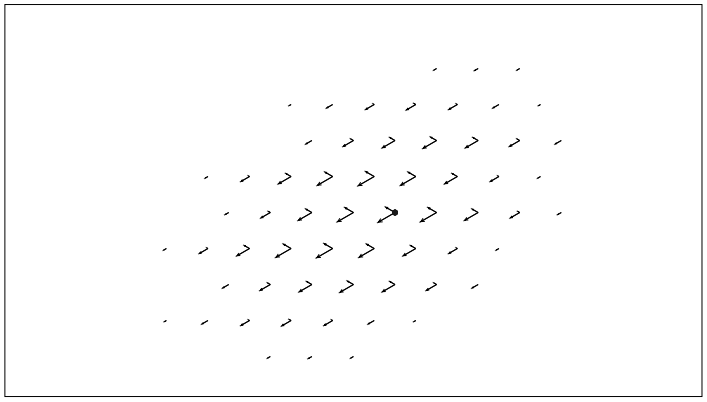

Figure 4.9 Kernel diagram for the experiment yielding the stripes organization.

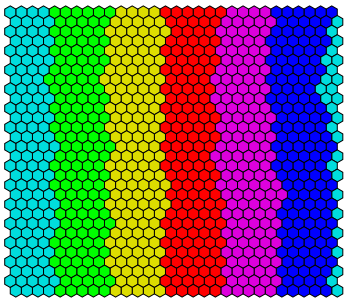

Figure 4.10 Orientation preference map for the stripes organization.

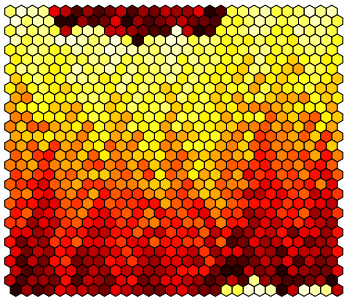

Figure 4.11 Spatial position map (x-axis) for the stripes organization. We observe a nearly continuous organization.

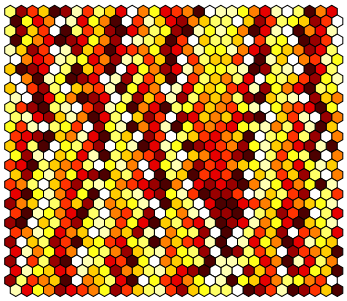

Figure 4.12 Spatial position map (y-axis) for the stripes organization.

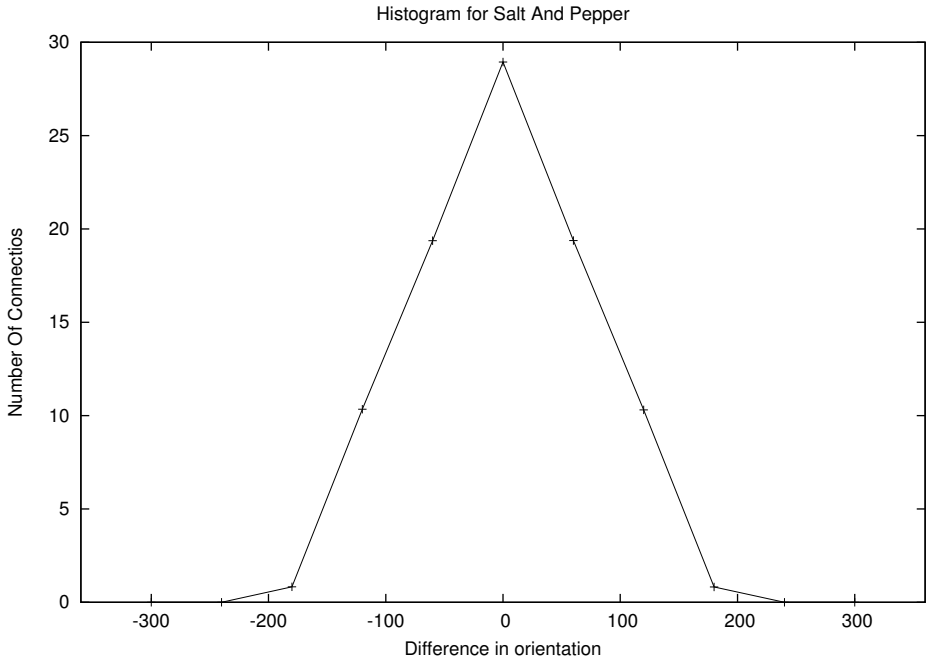

Figure 4.13 Number of connections vs. orientation difference with connecting simple cell for the salt and pepper organization.

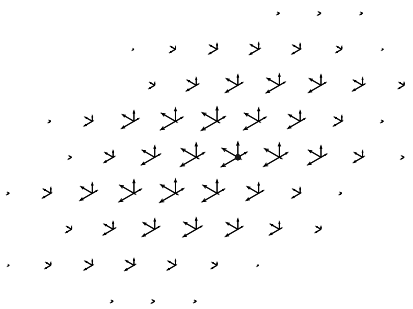

Figure 4.14 Kernel diagram for the experiment yielding the salt and pepper organization.

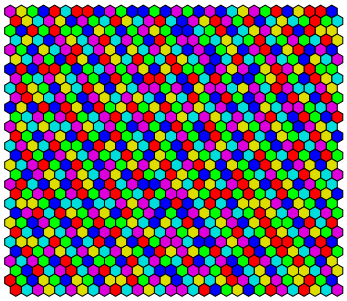

Figure 4.15 Orientation preference map for salt and pepper organization.

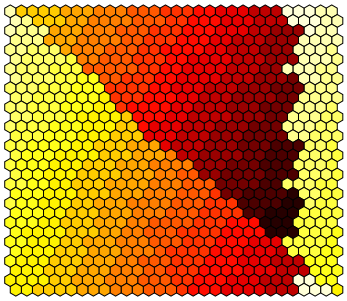

Figure 4.16 Spatial position map (x axis) for salt and pepper organization. We observe the continuous organization.

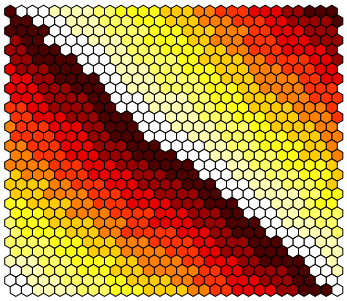

Figure 4.17 Spatial position map (y axis) for salt and pepper organization. We observe the continuous organization.

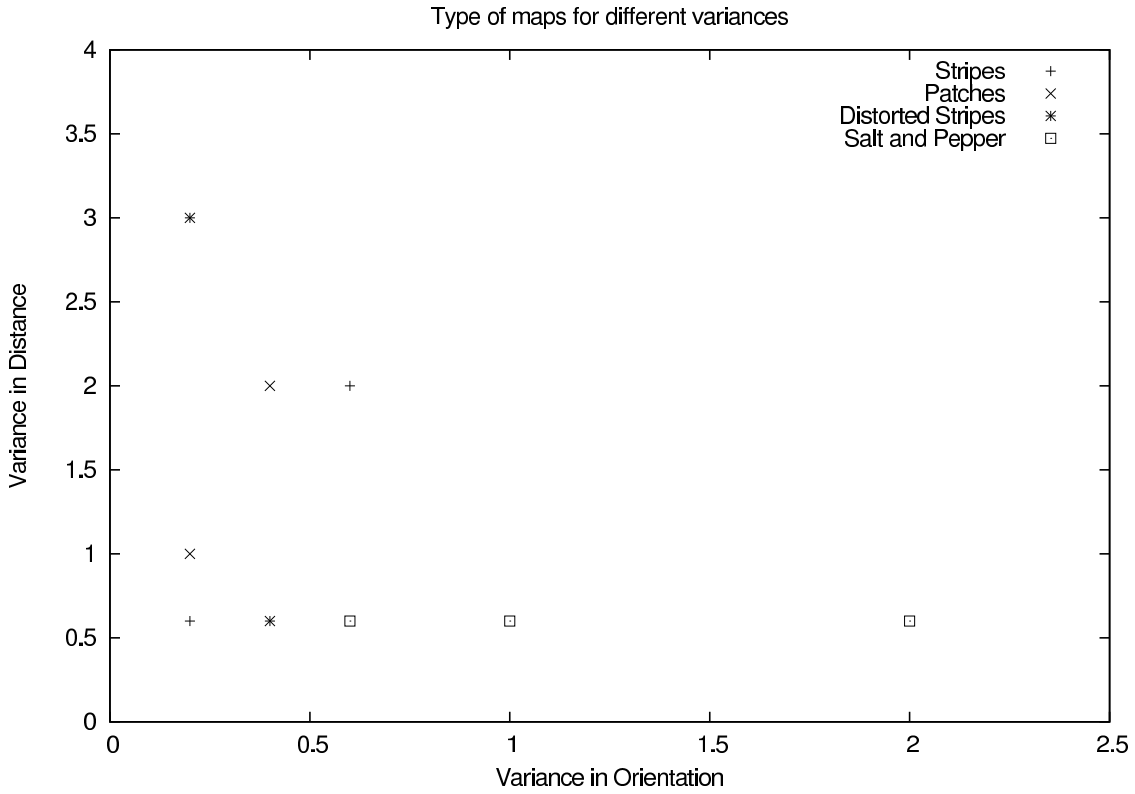

Figure 4.18 Graph displaying different orientation preference map organizations for different values of ${\sigma_\theta}^2$ and ${\sigma_x}^2 = {\sigma_y}^2$, determining the cortical circuit.

Chapter 5

Experiments and results

5.1 Setup

The basic theory has already been discussed in Section 4.2. In brief, the simple cells are connected to each other using the connection function described in Section 4.2. This *cortical circuit* is then embedded on the cortical space. Simulated annealing using the Metropolis algorithm is used to find the optimal embedding of the cortical circuit in the cortical space. This results in orientation and spatial preference maps.

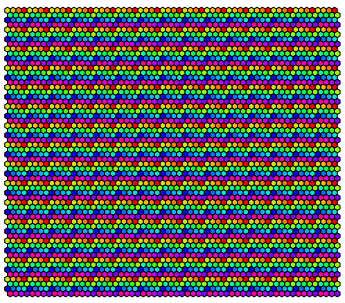

Figure 5.1 Initial orientation preference map.

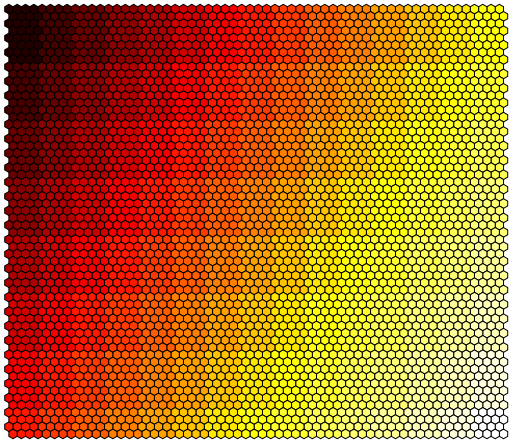

Figure 5.2 Initial spatial preference map (x-axis).

A cortical space of 60 $\times$ 60 simple cells with 16 unique orientations and a visual space of 15 $\times$ 15 was used. It was observed that an initial embedding based on a continuous variation in transition of spatial preference produced a lower total wire length (system energy). Moreover, it is well established (also emphasized by [2]) that such spatial preference maps are found in the visual cortex. Therefore the cortical

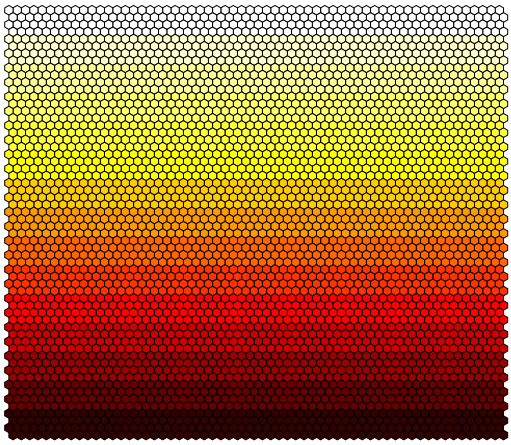

Figure 5.3 Initial spatial preference map (y-axis).

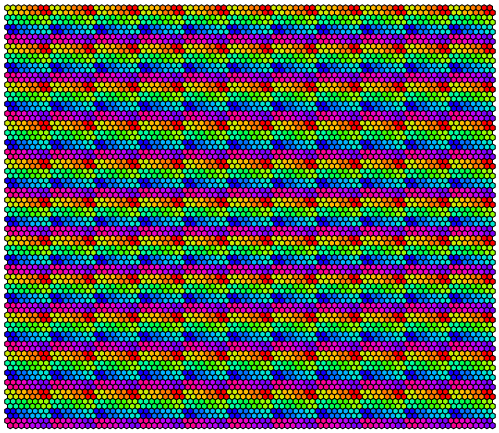

Figure 5.4 Initial orientation preference map for the cloned circuit.

circuit was initially embedded such that the spatial preference varied continuously in the x and y dimensions. Figure 5.1 shows the preference maps before the annealing process. Since simulated annealing changes the initial embedding, the simple cell swaps were limited to simple cells with similar spatial preference parameters.

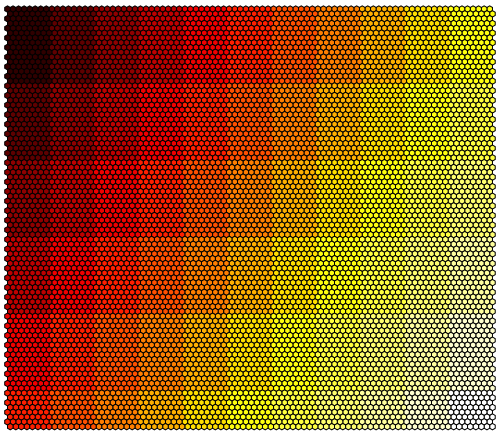

Figure 5.5 Initial spatial preference map (x-axis) for the cloned circuit.

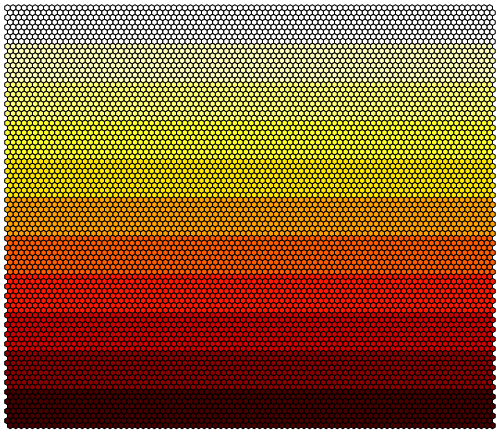

Figure 5.6 Initial spatial preference map (y-axis) for the cloned circuit.

5.1.1 Cloning

With the above experimental setup, one of the important results (Section 5.2) was an organization, that we termed *proto-pinwheel* for the orientation preference map. It is observed that, in the proto-pinwheel organization, there is only one cell with a specific combination of orientation and spatial preference. Hence, it is not possible for the orientation preference map to exhibit iso-orientation domians containing more than one simple cell. For this reason, we considered a cortical circuit where multiple cells possess the same combination of orientation and spatial preference parameter. These are termed *clones*. It was hoped that, with four clones, this would result in orientation preference maps exhibiting pinwheels connected by iso-orientation domains consisting of equivalence classes of clones. Results for this cloned circuit are described in Section 5.2.1

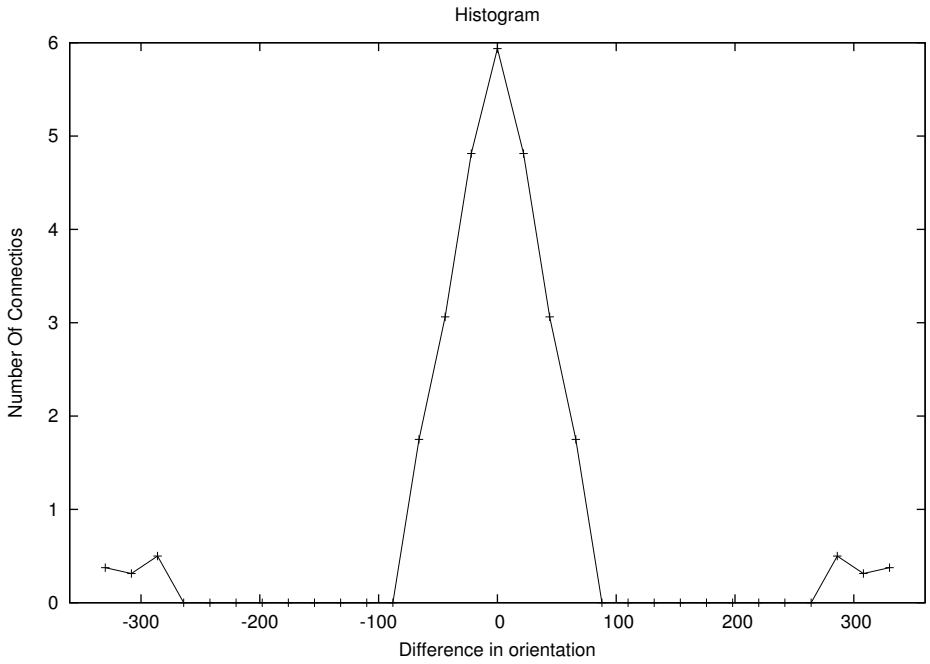

Figure 5.7 Connection histogram for the stripes orientation preference organization.

5.2 Results

Three type of orientation organization were observed namely: *stripes, pinwheel, and proto-pinwheels.* Figures 5.7-5.11 exhibits our results for the stripes orientation preference map. Figures 5.12-5.16 exhibits our results for the pinwheel-like orientation preference map. Figures 5.17-5.21 exhibits our results for the proto-pinwheel-like orientation preference map.

- **Stripes:** Figures 5.7-5.11 exhibits the characteristics of a vertical stripe orientation preference map. As observed from the histogram, a simple cell has relatively more connections with orientations closer to its own, than with different orientations. This is similar to the connection property for stripes organization in the Gaussian case. The spatial preference map for the x-axis seems to

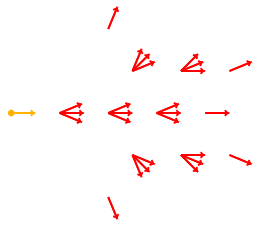

Figure 5.8 Kernel diagram used in the experiment yeilding stripes organization.

be forming horizontal stripes but the spatial preference map for the y-axis is random. Therefore, it seems that continuity is maximized for the x-axis and orientation parameter.

- **Pinwheel:** Figures 5.12-5.16 exhibits the characteristics of a pinwheel organization for the orientation preference map. The shape of the histogram seems

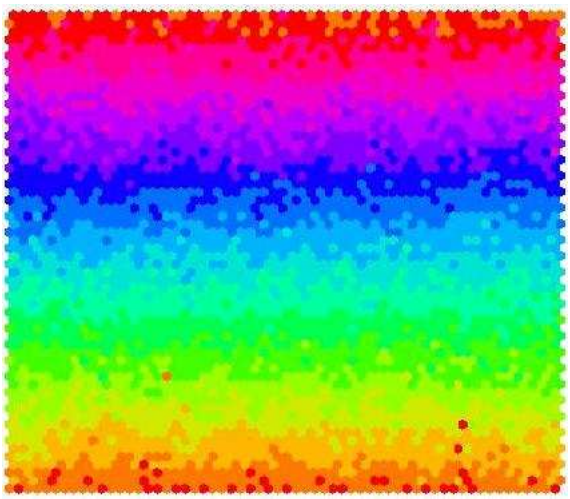

Figure 5.9 Orientation preference map for the stripes organization.

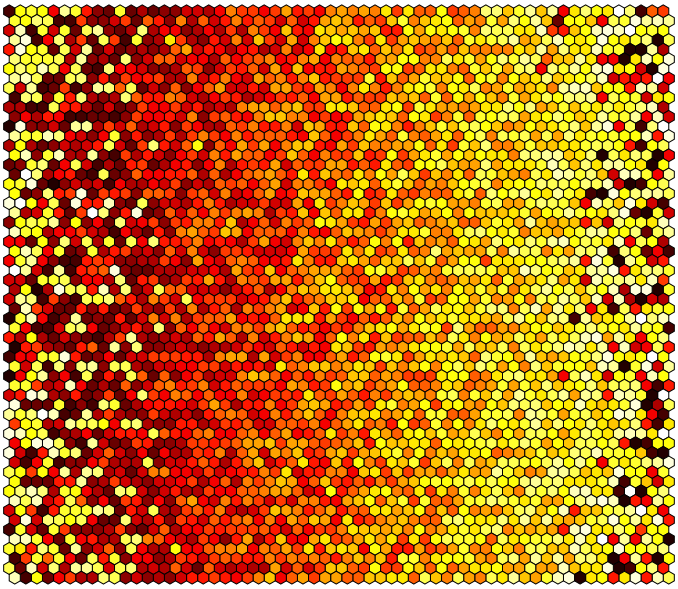

Figure 5.10 Spatial preference map (x-axis) for the stripes organization. We observe a vertical stripes organization.

similar to that for the stripes organization (Figure 5.7) but the number of connection for each orientation difference is much higher than for the stripes organzation. We conjecture that this is due to the larger kernel (Figure 5.13) used in this experiment as compared to the kernel used in the experiment which yielded stripes organization. The pin wheel structure has distinct iso-orientation domains and displays the opposite spin property of adjacent pinwheels like the orientation preference structure in visual cortex. This layout might be a result of the toroidal geometry used in our experiment, since each pinwheel is located in the corner and the iso-orientation domains join at corners. The symmetry of the pattern also suggests that this is the case. Finally, we observe that the spatial preference maps are not continuous, unlike those in visual cortex.

- **Proto-Pinwheel:** Figures 5.17-5.21 exhibits the characteristics of the proto-pinwheel organization for orientation preference map. The shape of the his-

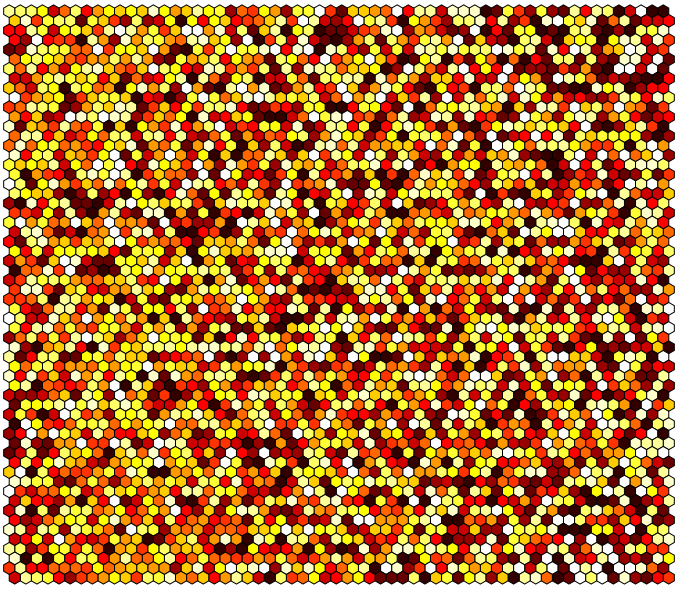

Figure 5.11 Spatial preference map (y-axis) for the stripes organization.

togram seems similar to the histogram for the stripes and pinwheel organizations. However, the number of connections have increased, in-spite of the fact that a smaller kernel was used. Close observation also suggests that the orientation preference map has multiple pinwheels with iso-orientation domain consisting of a single simple cell. The spatial preference map exhibits stripes layout. It seems that, similar to the Gaussian case the optimization process is maximizing the continuity of spatial preference parameters, but the regular structure of the orientation preference map suggests that orientation is playing a role unlike in the case of the salt and pepper organization. The hypothesis that the iso-orientation equivalence classes of a single simple cell suggests that clones of simple cells will tend to group together and form larger iso-orientation domains. This idea is explored further in Section 5.2.1

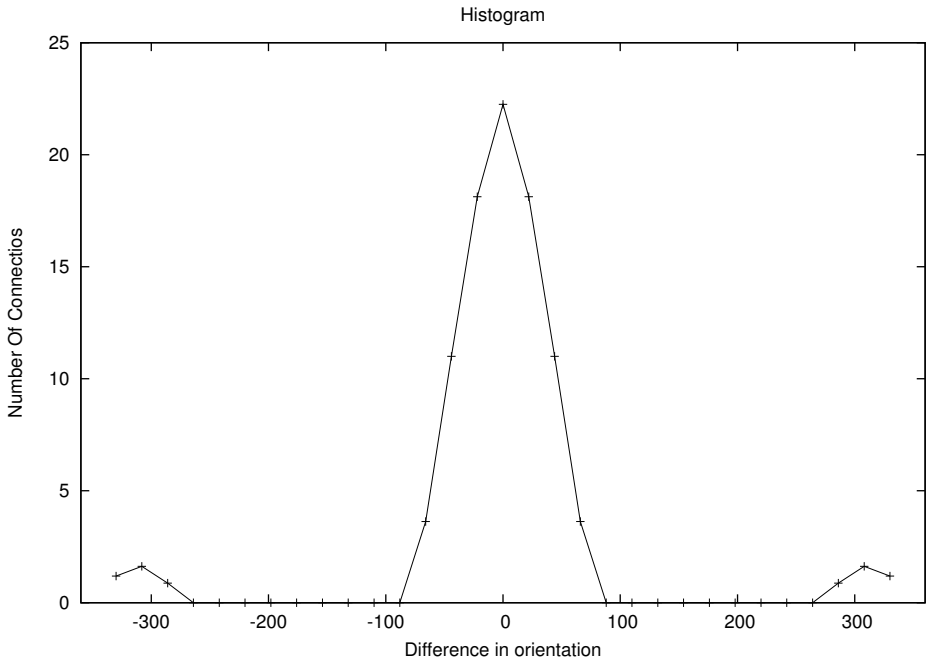

Figure 5.12 Connection histogram for the pinwheel organization.

5.2.1 Results with cloned circuits

Figures 5.22-5.26 exhibits the results of optimizing the cortical containing the cloned simple cells. Due to the presence of the redundant clones in the circuit, the histogram

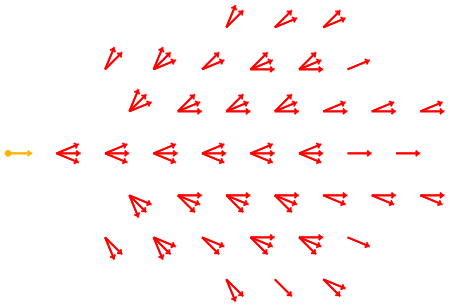

Figure 5.13 Kernel diagram used in the experiment yielding pinwheel organization.

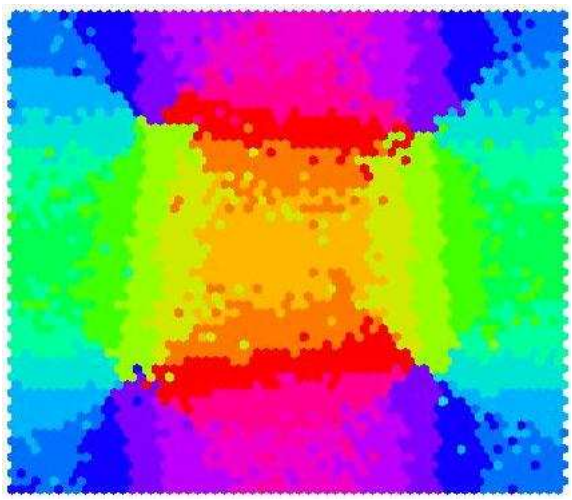

Figure 5.14 Orientation preference map for the pinwheel organization.

shows a relatively larger number of connections. The orientation preference map

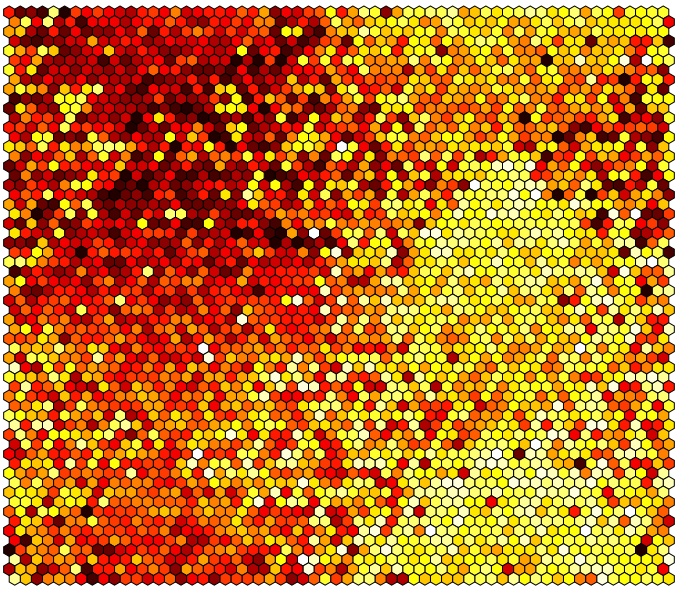

Figure 5.15 Spatial preference map (x-axis) for the pinwheel organization.

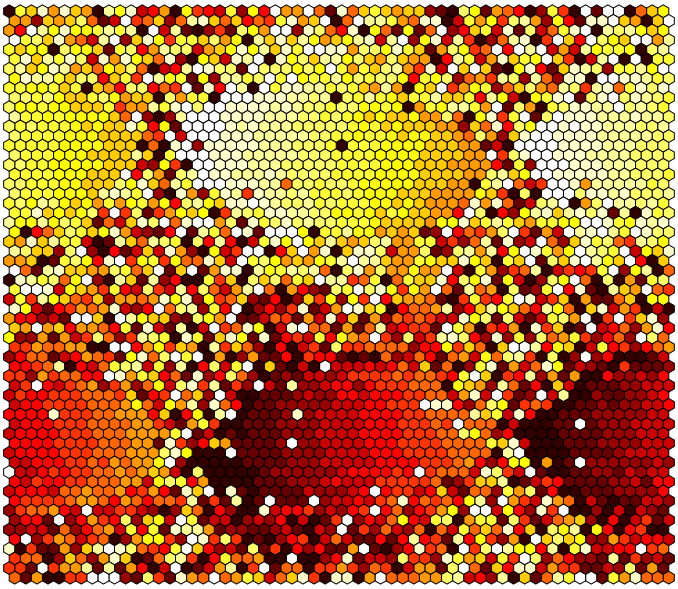

Figure 5.16 Spatial preference map (y-axis) for the pinwheel organization.

shows many more pinwheels than in the organization shown in Figure 5.14. It is also interesting to note that all of the pinwheels have the same spin sign. This seems to be the result of using hexagonal coordinate system to sample the visual space. Since the hexagonal tesselation is not 2-colorable, it is not possible to come up with an assignment for the pinwheel spins, with adjacent pinwheel having opposite sign. It is not surprising that the spatial preference organization is continuous (Figures 5.15 and 5.16). Moreover, spatial preference organization is similar to the organization observed in the proto-pinwheel result.

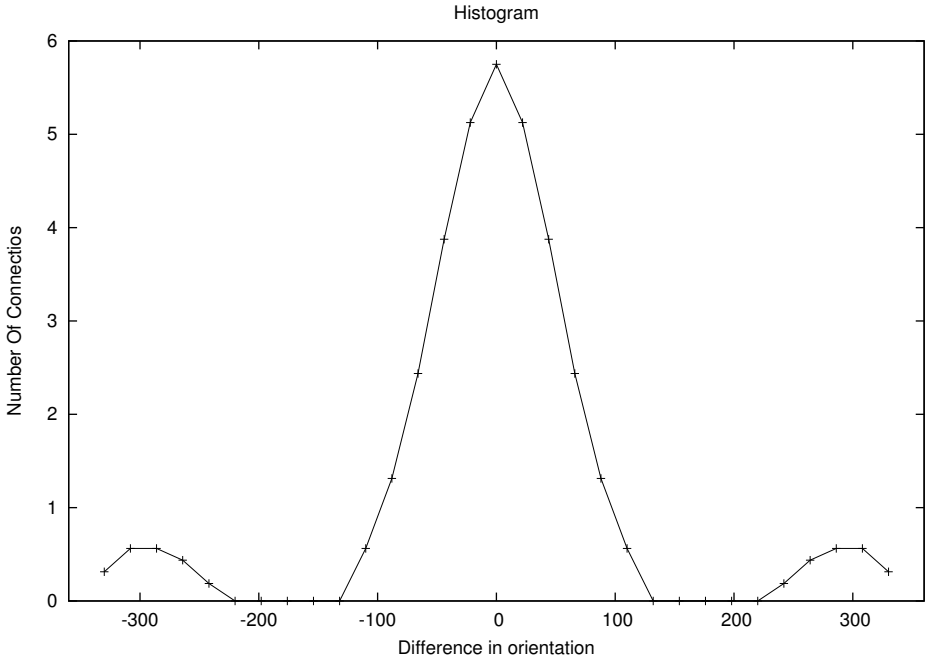

Figure 5.17 Connection histogram for the proto-pinwheel organization.

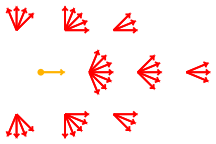

Figure 5.18 Kernel diagram used in experiment yielding proto-pinwheel organization.

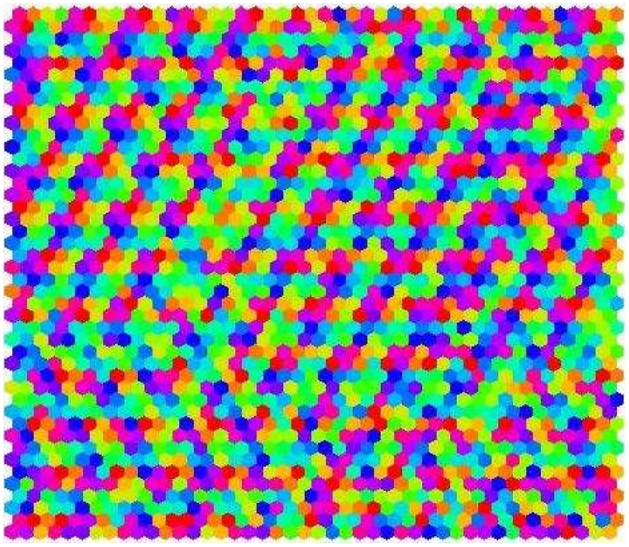

Figure 5.19 Orientation preference map for the proto-pinwheel organization.

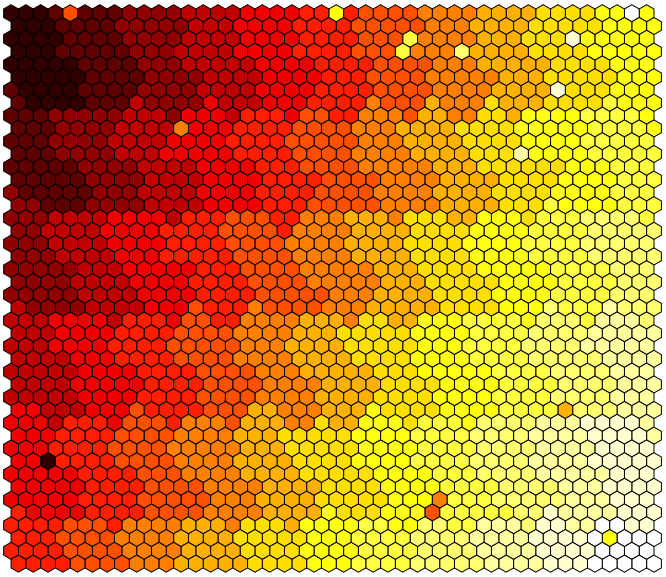

Figure 5.20 Spatial preference map (x-axis) for the proto-pinwheel organization.

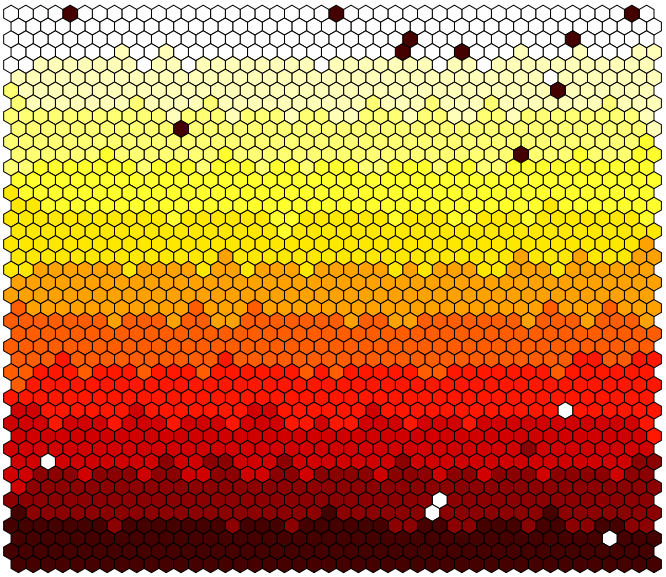

Figure 5.21 Spatial preference map (y-axis) for the proto-pinwheel organization.

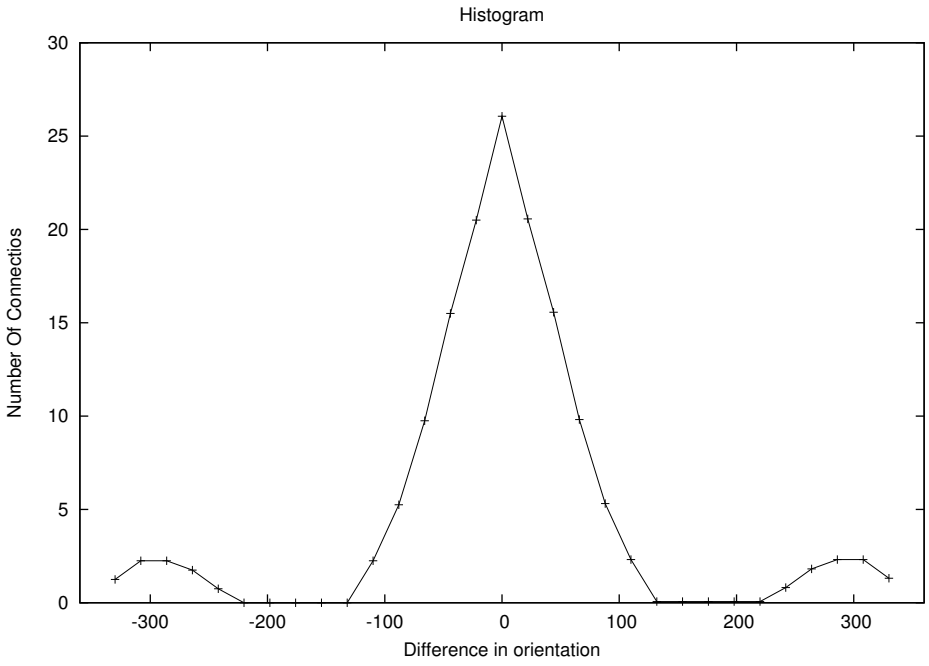

Figure 5.22 Connectiom histogram for the pinwheel organization of the cloned circuit.

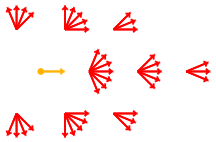

Figure 5.23 Kernel diagram used in the experiment yielding the pinwheel organization of the cloned circuit.

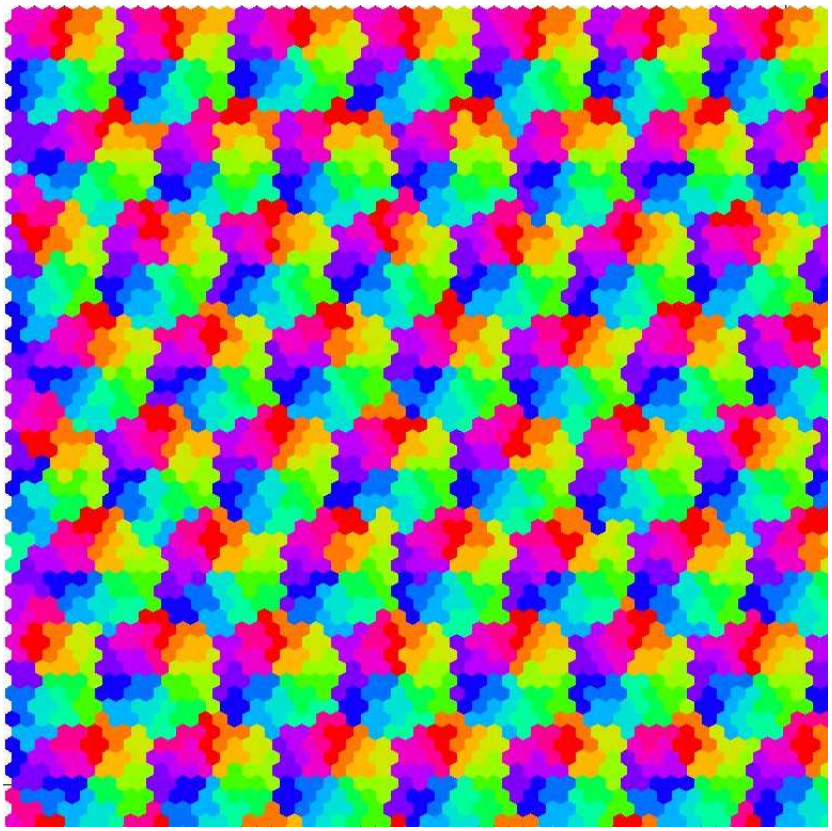

Figure 5.24 Orientation preference map for the pinwheel organization of the cloned circuit.

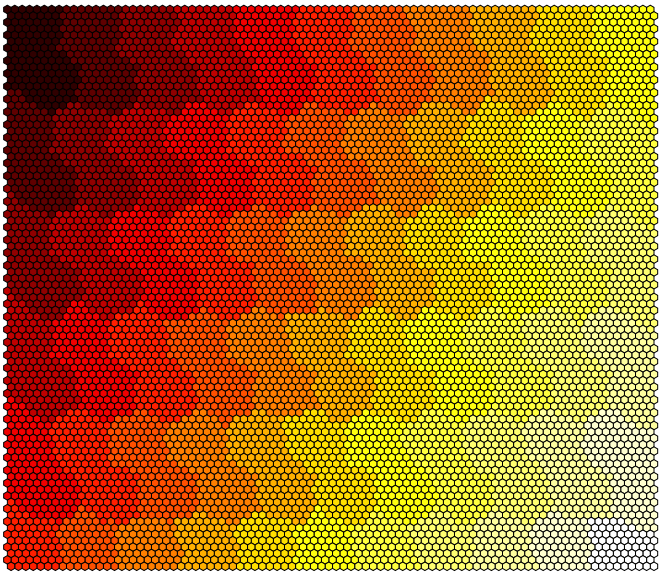

Figure 5.25 Spatial Preference map (x-axis) for the pinwheel organization of the cloned circuit.

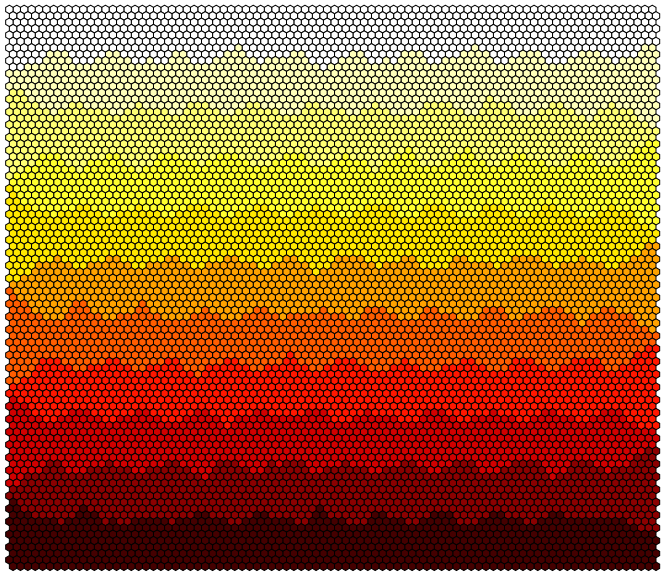

Figure 5.26 Spatial Preference map (y-axis) for the pinwheel organization of the cloned circuit.

Chapter 6

Conclusion and Future Work

The orgins of the pinwheel structure which is charateristic of orientation preference map in human visual cortex has been actively researched. It has been hypothesized that the neurons in the visual cortex could be preforming a computation related to contour completion. Suggestive orientation preference maps like the pinwheel and the cloned proto-pinwheel organizations, which we have observed in our experiments, are in some ways similar to the real maps but are either too regular or lack the opposite spin property. It seems that an approach of increasing the visual space of the system for th eexperiment yielding pinwheel like organization or reducing the kernel might increase the number of pinwheels in layout of the cortical circuit. Since this organization has the correct spin property, it is hypothesized that this might result in a better orientation preference map. The disadvantage with this approach is that the spatial preference maps are not continuous, as observed in visual cortex. An approach using a rectangular sampling pattern for the visual space might create a configuration of pinwheels which is 2-colorable. coordinate system might help in breaking the inherent symmetry of above described results for proto-pinwheel organization and in the process might also induce the opposite spin with the adjacent pinwheels.

References

[1] Blasdel G. G., Orientation selectivity, preference and continuity in monkey striate cortex, *J. Neuroscience* **7**, pp. 1414-1427, 1987.

[2] Crick Francis, *The Astonishing Hypothesis: The Scientific Search for the Soul*, Touchstone, New York, 1995.

[3] Daugman John G., Uncertainity relation for resolution in space, spatial frequency, and orientation optimized by two-dimensional visual cortical filters, *J. Opt. Soc. Am. A* **7** (2), pp. 1160-1169, 1985.

[4] Durbin Richard and Mitchison Graeme, A dimension reduction framework for understanding cortical maps, *Nature* **343**, pp. 644-647, 1990.

[5] Grossberg S., Mingolla E., Neural dynamics of form perception: Boundary completion, and illusory figures, and neon color spreading, *Psychological Review* **92**, pp. 173-211, 1985.

[6] Horn, B. K. P., The curve of least energy. (MIT AI La Memo No. 612), Cambridge, MA:MIT.

[7] Hubel D. H., Wiesel T. N., Receptive fields of single neurones in the cat's striate cortex, *J. Physiol.* **150**, pp. 91-104, 1959.

[8] Hubel D. H., Wiesel T. N., Receptive fields and functional architecture of the monkey striate cortex, *J. Physiol.* **195**, pp. 215-243, 1962.

[9] Kirkpatrick, S., Gelatt, C. D., and Vecchi, M. P., Optimization by simulated annealing, *Science* **220**, pp. 671-680, 1983.

[10] Koulakov, A. Alexei and Chklovskii B. Dimitri, Orientation preference patterns in mammalian cortex: A wire length minimization approach, *Neuron* **29**, pp. 519-527, 2001.

[11] Maldonado, P. E., Gdecke I., Gray C. M., Bonhoeffer T., Orientation selectivity in pinwheel centers in cat striate cortex, *Science* **276**, pp. 1551-1555, 1997.

[12] Marr David, *Vision: A Computational Investigation into the Human Representation and Processing of Visual Information*, W. H. Freemon and Company, New York, 1996.

[13] Metropolis N., Rosenbluth M. N. and Teller, A. H., Equation of state calculations by fast computing machines, *J. Chem. Phys* **21**, pp. 1087-1092, 1953.

[14] Parent P. and Zucker S., Trace inference, curvature consistency and curve detection, *IEEE Transactions on Pattern Analysis and Machine Intelligence* **11**, pp. 1551-1555, 1997.

[15] Snyder Wesley E., Qi Hairong and Sander William, *Center for Advanced Computing Communication.*

[16] Swindale V. Nicholos, Shoham Doron, Grinvald Amiram, Bonhoeffer Tobias and Hubbener Mark, Visual cortex maps are optimized for uniform coverage, *Nature Neurosience* **3** (8), pp. 822-826, 2000.

[17] Swindale V. Nicholas, Looking into a Klein bottle, *Current Biology* **6** (7), pp. 776-779, 1996.

[18] Williams R. Lance, Jacobs David W., Stochastic completion fields: A neural model of illusory conrtour shape and salience, *Neural Computation* **9** (4), pp. 837-858, 1997.

[19] Williams R. Lance, Jacobs David W., Local parallel computation of stochastic completion fields, *Neural Computation* **9** (4), pp. 859-881, 1997.

[20] *http://csep1.phy.ornl.gov/CSEP/MO/NODE28.html*, 15 April, 2004.

[21] *http://www.cshl.org/gradschool/chklovskii.html*, 15 April 2004.

[22] *http://www.biols.susx.ac.uk/home/GeorgeMather/LinkedPages/Physiol/Cortex.html*, 15 April 2004.

[23] *http://ifcsun1.ifisiol.unam.mx/Brain/cercox.htm*, 15 April 2004.